

CHAPTER FORTY FOUR

CALIBRATION AND VERIFICATION OF A DISSIPATION MODEL FOR RANDOM BREAKING WAVES

J.A. Battjes* and M.J.F. Stive**

ABSTRACT

A model describing the average rate of energy dissipation in random waves breaking in shallow water, published previously by the first author and Janssen (1978), has been applied to an extensive set of data for the purposes of calibration and verification. Both laboratory and field data were used, obtained on beaches with a more or less plane slope as well as on barred beaches, and for a wide range of wave conditions. Optimal values have been estimated for an adjustable breaking waveheight-coefficient in the model; these appear to vary slightly but systematically with the incident wave steepness, in a range which is physically realistic. A parameterization of this dependence allows the use of the model for prediction. Applied to the present data set, the correlation coefficient between measured and predicted rms wave heights is 0.98, with an rms normalized error of 6% and a bias which does not differ significantly from zero.

1. INTRODUCTION

The principal physical process in the surfzone is the dissipation of the energy of incident windwaves and swell, due to wave breaking. Because of the randomness of wind-generated waves the occurrence of breaking at a fixed location is itself a random process. Realistic models for the prediction of the onshore variation of wave energy and radiation stress should take this randomness into account.

Battjes and Janssen (1978), hereafter referred to as BJ, presented an approach in which the mean local rate of energy dissipation is modelled, based on that occurring in a bore and on the local probability of wave breaking. The result is used as a sink in the energy balance, which is subsequently integrated to obtain the wave energy as a function of onshore distance. A few laboratory experiments performed by BJ, including cases with a bar-trough profile, indicated a very promising degree of agreement.

Thornton and Guza (1983) have presented a refinement of BJ's model, which however has negligible consequences for the predicted rms-variation. They also made a comparison between calculated and measured rms wave heights, using field data of low swell incident on a gently sloping, almost plane beach. Again, good agreement was found, with an rms relative error of about 9%.

* Delft University of Technology, Delft, the Netherlands

** Delft Hydraulics Laboratory, Delft, the Netherlands

The range of bottom profiles and incident wave parameters in the measurements referred to above is too restricted to allow a systematic investigation of the model performance and of the optimum values of the adjustable parameters. It was therefore decided to carry out an extensive calibration and verification of the model. The present paper briefly presents the results of this investigation. A full account will be published elsewhere.

The paper is made up as follows. A resume of BJ's model is given first. Then the observational conditions and procedures are described. The results are used for estimation of adjustable model coefficients as a function of the independent parameters (particularly the incident wave steepness). Finally, an overall assessment of the model performance with parameterized coefficients is presented, followed by a discussion.

2. RESUME OF BATTJES AND JANSSEN'S MODEL

In this section, we present a summary of BJ's model for reference in the remainder of this paper.

The essence of BJ's model is the estimation of the time-averaged rate of dissipation of wave energy per unit area due to breaking (\bar{D}). Two aspects are distinguished: the rate of energy dissipation in periodic breaking waves, and the probability of occurrence of breaking waves of given height in a random wave field.

The energy dissipation in breaking waves is modelled after that in a bore of the same height. For periodic waves with frequency f and breaking waveheight H_b in water of mean depth h , BJ arrive at the following order-of-magnitude estimate for the mean dissipation rate per unit area:

$$D \sim \frac{1}{2} f \rho g H_b^2 \quad (1)$$

For application to random waves, the expected value of D (written as \bar{D}) must be estimated, taking into account the randomness of the waves and the fact that not all the waves passing the point considered are breaking. In this estimate, BJ have used characteristic values for the frequency and the breaking waveheights, and they have derived a prognostic equation for the local fraction of breaking waves.

The characteristic frequency used in the following is f_p , the frequency at the peak of the energy spectrum of the incident waves.

The mean square of H_b is equated by BJ to the square of the nominal, depth-limited height of periodic waves (H_m) in water of the local mean depth. BJ use a Miche-type expression for H_m , adapted through the inclusion of a parameter γ to account for influences of bottom slope and mean wave steepness:

$$H_m = 0.88 k_p^{-1} \tanh(\gamma k_p h / 0.88) \quad (2)$$

in which $k_p = 2\pi/L_p$ is the wavenumber calculated on the basis of the linear theory dispersion equation for gravity waves with frequency f_p .

To determine the local fraction of breaking waves (Q), BJ assume that the cumulative probability distribution of all waveheights (breaking or non-breaking) is of the Rayleigh-type, cut off discontinuously at $H = H_m$. This was shown to imply the following relation between Q and H_{rms}/H_m , in which H_{rms} is the rms of all waveheights:

$$\frac{1 - Q}{-\ln Q} = \left(\frac{H_{rms}}{H_m} \right)^2 \quad (3)$$

Substituting the approximations mentioned above in the averaged equation (1), and writing the order-of-magnitude relation in the form of an equation, gives

$$\bar{D} = \frac{1}{4} \alpha Q f_p \rho g H_m^2 \quad (4)$$

in which α is a coefficient which is expected to be of order 1. It is pointed out that \bar{D} varies with H_{rms} through Q .

To close the model, \bar{D} is used as a sink in the wave energy balance, which in its most reduced form (statistically steady, uniform alongshore, no other sources or sinks than \bar{D}) can be written as

$$\frac{\partial P_x}{\partial x} + \bar{D} = 0 \quad (5)$$

P_x is the onshore energy flux per unit width, approximated as $E c_g$, in which $E = \frac{1}{8} \rho g H_{rms}^2$ and c_g is the group velocity according to the linear theory for $f = f_D$.

The energy balance (5) is integrated simultaneously with the balance of onshore momentum (not reproduced here), resulting in the simultaneous determination of the onshore variation of H_{rms} and of the set-up of the mean water level ($\bar{\eta}$).

3. OBSERVATIONS

Empirical data from various sources have been collected for calibration and verification of the theoretical model. These include laboratory data and field data, obtained for a variety of wave conditions and bottom profiles. The original data of BJ are included also.

All laboratory data used herein have been collected in wave flumes, using mechanically generated random waves. The field sites and conditions were selected so as to have more or less statistically uniform conditions alongshore and normal incidence (for the principal wave propagation direction). Direct wind influence was negligible in all cases considered here except one.

The laboratory bottom profiles include plane slopes and a schematized bar-profile in concrete, as well as concave and barred profiles in sand. Two field sites on the Dutch coast were used, one on a beach near Egmond, the other on a shoal in the mouth of the Haringvliet estuary. The beach has a typical double bar system. The measurements in the Haringvliet estuary were conducted in a line across an elongated shoal, with more or less parallel depth contours over a distance of about 5000 m. The minimum depth over the shoal is 0.1 m below Mean Sea Level, and about 1.5 m below Mean High Water Level.

For each combination of incident waves and bottom profile, measurements were made of the bottom profile, the mean water level, the rms wave height and the peak frequency at an offshore reference point, and the rms wave heights at various points in the profile. In some cases the variation of mean water level with distance onshore was measured also. The surface elevation signals were analyzed to estimate the variance, σ^2 , and its spectral distribution. The measured variances were used to estimate H_{rms} according to

$$H_{rms} = 8^{\frac{1}{2}} \sigma. \quad (6)$$

A resume of the independent parameters is given in Table 1. The columns 4, 5 and 6 list the values of h , H_{rms} and f_p in the offshore reference point (indicated with the subscript r). Values of a mean deep-water wave steepness $s_o = H_{rms}/L_{op}$ are listed in column 7, based on $L_{op} \equiv g/(2\pi f_p^2)$ and a deep-water value of H_{rms} calculated from the values in the reference point using linear shoaling theory for periodic waves with frequency f_p , i.e. $H_{rms}_o = H_{rms}_r (c_{gr}/c_{go})^{\frac{1}{2}}$. The parameter $\hat{\gamma}$ in column 8 will be explained below.

(1)	(2)	(3)	(4)	(5)	(6)	(7)	(8)
Nr.	Source	Profile [m]	h_r [m]	H_{rms_r} [Hz]	f_{p_r} -	s_o -	$\hat{\gamma}$
1	Battjes and Janssen (1978)	Plane (1:20)	.705	.144	.511	.026	0.73
2			.697	.122	.383	.012	0.60
3			.701	.143	.435	.018	0.70
4	Battjes and Janssen (1978)	Schematized bar-trough	.703	.137	.450	.019	0.72
5			.645	.121	.443	.016	0.69
6			.763	.104	.467	.016	0.70
7			.732	.118	.481	.019	0.70
8			.616	.143	.498	.024	0.72
9	Stive (1984)	Plane (1:40)	.700	.138	.341	.010	0.62
10			.700	.136	.633	.038	0.81
11			4.19	1.00	.185	.023	0.82
12	Van Overeem (1983)	Concave	.800	.211	.392	.022	0.73
13			.800	.096	.568	.022	0.80
14			.800	.132	.559	.029	0.80
15	Van Overeem (1983)	Bar-trough	.800	.132	.557	.029	0.83
16			.800	.212	.393	.022	0.75
17	Derks and Stive (1984)	Bar-trough	10.80	1.29	.157	.022	0.67
18			15.65	2.78	.115	.026	0.73
19	Dingemans (1983)	Bar	16.40	.94	.143	.013	0.70
20			11.10	2.43	.128	.028	0.82

Table 1 Experimental and environmental parameters; cases 1...16 laboratory experiments, cases 17...20 field experiments

4. MODEL CALIBRATION

The energy balance and the momentum balance have been numerically integrated with respect to the onshore distance (x) for each case listed in Table 1, using chosen values of (α, γ) . The peak frequency f_p and the coefficients (α, γ) were kept constant with respect to x . Each integration gives two functions $\eta(x)$ and $H_{rms}(x)$ shoreward of the reference point, which can be compared to the measurements. Repeating the integration for several choices of (α, γ) , optimal values of these coefficients have been estimated, such that a maximum agreement is obtained between computed and measured H_{rms} values.

The coefficients α and γ can formally be varied independently of each other. However, in the calibration process just described there is a dependence between the two since in this process the model is forced to simulate a certain energy dissipation, which depends on α and γ through its proportionality to the product $\alpha Q H_m^2$ (see eq. 4). Therefore, there is effectively only one degree of freedom in tuning the model to a measured waveheight variation. The calibration was in fact carried out by estimating optimal values of γ (denoted as $\hat{\gamma}$) under the constraint $\alpha = 1$. The resulting values of $\hat{\gamma}$ are listed in column 8 of Table 1. They fall in the range from 0.60 to 0.83, which is physically realistic.

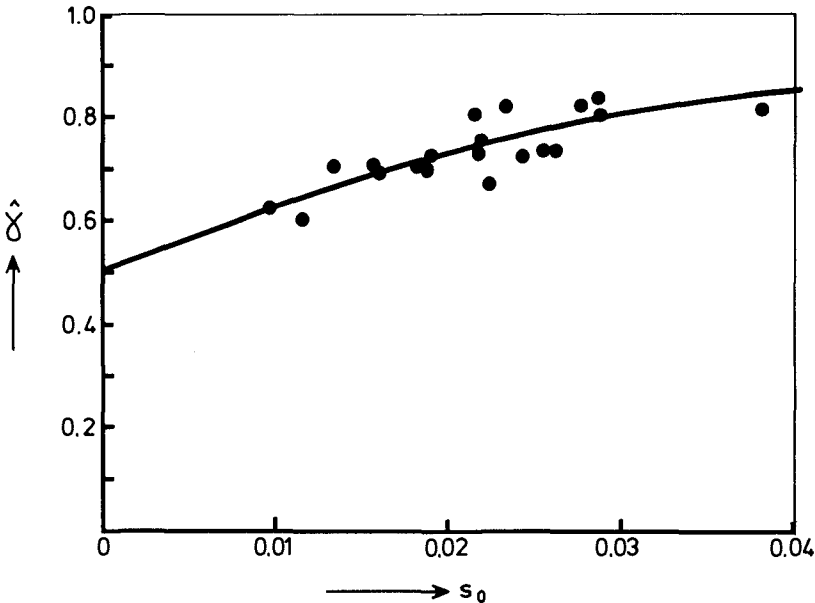


Fig. 1 Estimated values of breaker height coefficient $\hat{\gamma}$ vs. deep-water steepness s_0 ; data points: optimal value per case; full curve parameterization given by eq. 7.

It is known that the process of wave breaking in shallow water is influenced by the incident wave steepness and by the bottom slope. It was therefore investigated whether the estimated $\hat{\gamma}$ -values varied systematically with these parameters. No significant variation of $\hat{\gamma}$ with beach slope could be found. However, there did appear to be a systematic dependence of $\hat{\gamma}$ on the deep-water steepness s_0 , as can be seen in Fig. 1. A tanh-function has been fitted to these data, with the result

$$\hat{\gamma} = 0.5 + 0.4 \tanh(33 s_0) \quad (7)$$

This relation, indicated in Fig. 1 by the full line, can be used for purposes of prediction.

5. EVALUATION OF MODEL PERFORMANCE

In order to gain an impression of the overall performance of the model, we have applied it again to each of the 20 cases considered, this time using the parameterization (7) described above. The model was found to be quite realistic in the simulation of the observed rms waveheights. Some examples of the results are shown in the Figs. 2 through 4. A comparison of normalized computed and measured H_{rms} values in the zone of wave shoaling and breaking covering all 20 cases is given in Fig. 5. The correlation coefficient is 0.98; the model bias based on the best-fitting proportional relationship is 0.01, and the rms relative error, normalized with the mean value of all measured values of H_{rms}/H_{rms_0} shown in Fig. 5, is 0.06. These numbers confirm in a quantitative sense the high degree of realism possessed by the model for the prediction of the waveheight variation in areas of wave breaking. The good model performance is remarkable in view of the complexity of the physical processes involved, and the relatively simple concept on which the model is based.

The maximum set up also is well predicted (Fig. 2), but in areas of large set-up gradient the predicted rise is systematically too far seaward. This phenomenon has been noted previously by Battjes (1972) and by BJ. It suggests that the decrease in momentum flux lags behind the decrease in wave energy as measured through the variance of the surface elevation. A possible explanation for this phenomenon would be a relative surplus of kinetic energy in the area of intensive wave energy dissipation. This might consist partly of a surplus of kinetic wave energy (coherent with the surface elevation) and partly of turbulence energy. The latter possibility can be investigated by adding turbulent Reynolds stresses to the radiation stresses, e.g. on the basis of the model for turbulence in the surf zone presented by Battjes (1975). However this matter has not been pursued in the present study.

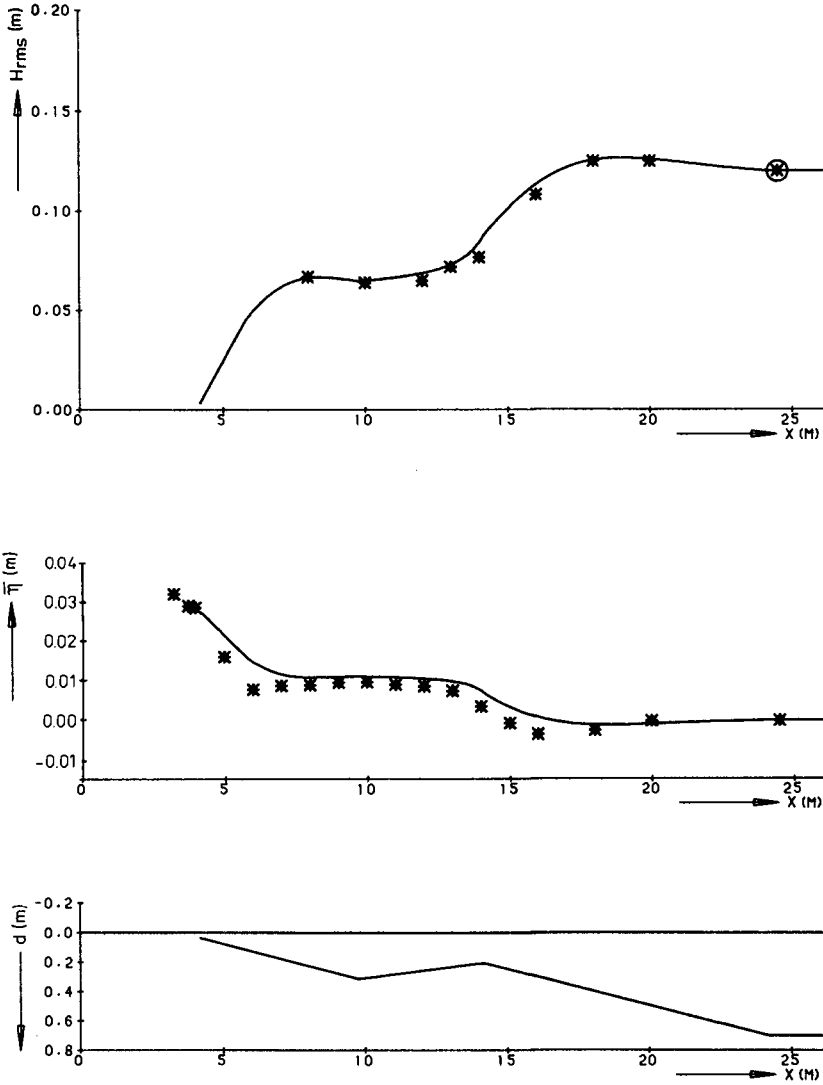


Fig. 2 Results for case 5 (laboratory); profiles of bottom elevation below MWL_r (d), mean water level above MWL_r ($\bar{\eta}$) and rms wave-height (H_{rms}) vs. distance normal to shore (x); data points: measured values with offshore reference value encircled; full curves: computed values of $\bar{\eta}$ and H_{rms} , based on parameterization of γ given by eq. 7.

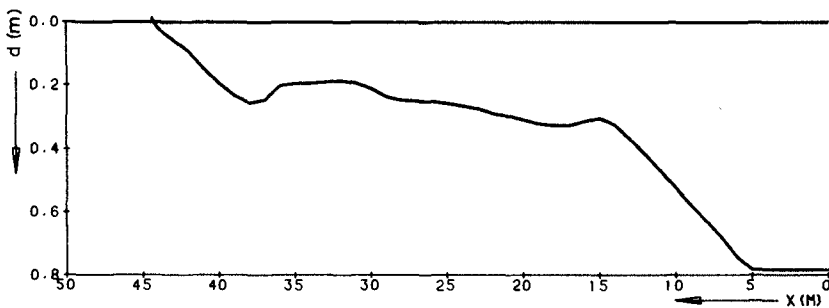
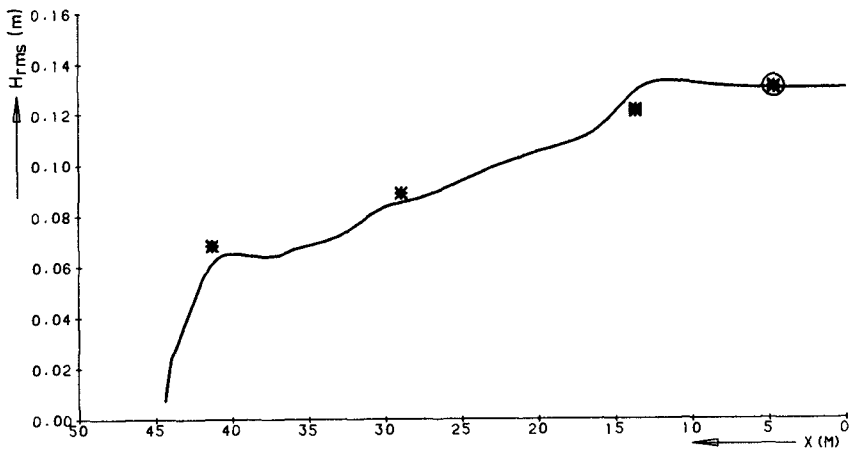


Fig. 3 Results for case 15 (laboratory); for legend see Fig. 3 (except $\bar{\eta}$).

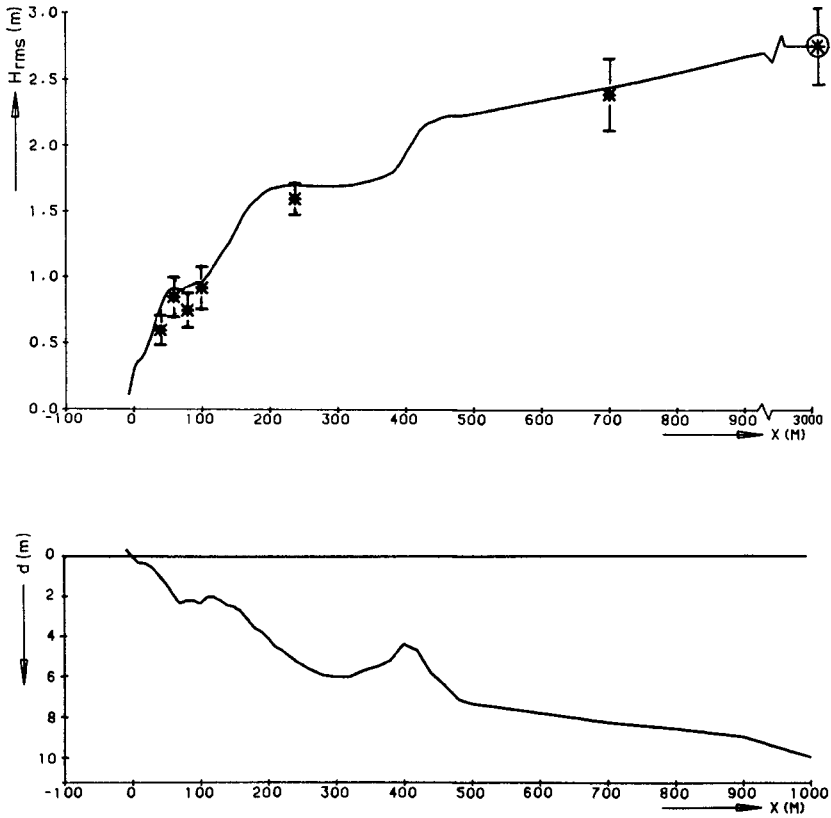


Fig. 4 Results for case 18 (field - Egmond beach); for legend see Fig. 3; the vertical line segments indicate one standard deviation on either side of the plotted data point.

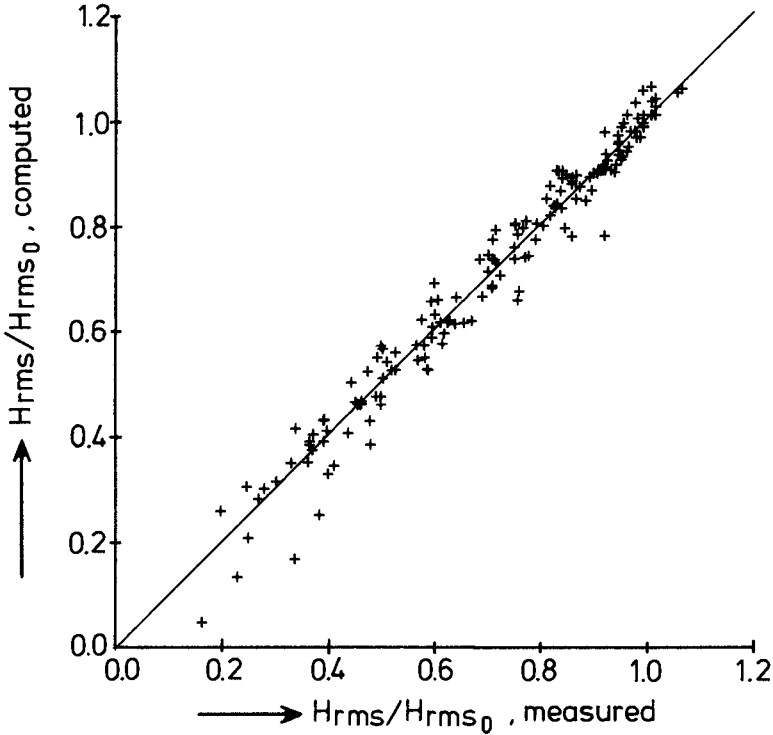


Fig. 5 Comparison of calculated and measured rms waveheights, normalized with the deep-water value. The calculated values are based on the parameterization given by eq. 7. The straight line is the least squares best-fit proportional relationship.

6. DISCUSSION

The model calibration described above is based on situations of one-dimensional wave propagation. However, the key element in the model is the estimate of the mean energy dissipation in random waves due to breaking, which is believed to apply equally well in cases of two-dimensional wave propagation.

In the situations used in the calibration described herein, there were no significant sources or sinks of energy between deep water and the surfzone. In these situations, a parameterization of the model coefficient(s) in terms of a characteristic deepwater wave steepness is meaningful, as in eq. 7. In applications, more complicated situations may arise, in which processes other than pure shoaling play a non-negligible role between deep water and the surfzone. Examples are

wave refraction, and energy dissipation in the near-bottom boundary layer. For such situations, we use the following procedure.

We distinguish areas of negligible breaking and areas of significant breaking. (In barred profiles, more than one area of significant breaking may occur). Somewhat arbitrarily, we define an area of significant breaking as the region of space (in the horizontal plane) where $H_{rms}/h > 0.25$. This corresponds roughly with $H_{rms}/H_m > 0.35$, approximately the limit above which the fraction of breaking waves is no longer negligible.

In a process of numerical integration along a wave ray in water of decreasing depth, in which refraction and various energy sources and sinks can be taken into account, the dissipation due to breaking is neglected as long as $H_{rms} < 0.25 h$. At the point where $H_{rms} = 0.25 h$, the local value of H_{rms} is converted to an equivalent deep-water value using linear shoaling only (i.e. $H_{rms_o} = (c_g/c_{g_o})^2 H_{rms}$). This value is used to determine $\hat{\gamma}$ according to eq. 7; the value of $\hat{\gamma}$ so obtained is used in the integration of the energy balance (including the dissipation due to breaking according to eq. 4) across the area of non-negligible breaking downwave of the point of transition (i.e., as long as $H_{rms}/h > 0.25$).

7. CONCLUSIONS

A calibration is performed of a theoretical model for the wave energy dissipation and resulting wave energy variation in random breaking waves. The theoretical model has effectively one adjustable parameter. Optimal values of this coefficient have been determined. These vary slightly in a physically realistic range with the incident wave steepness. A parameterization of this dependence is presented so that the model can be used for prediction. Using this parameterization, the overall performance of the model has been evaluated. The coefficient of correlation between predicted and observed H_{rms} -values is 0.98; the model bias is not significantly different from zero, and the rms relative error is 0.06. The maximum set-up of the mean water level also is well predicted.

ACKNOWLEDGEMENT

The authors wish to express their gratitude to H. Derks, M.W. Dingemans and J. van Overeem, who supplied additional information on the measurement results obtained by them in their respective studies. Furthermore M.W. Dingemans is thanked for his support in developing the numerical model.

REFERENCES

- BATTJES, J.A., Set-up due to irregular waves, in Proceedings of the 13th International Conference Coastal Engineering, pp. 1993-2004, American Society of Civil Engineers, New York, 1972.
- BATTJES, J.A., A turbulence model for the surf zone, in Proceedings Symposium on Modelling Techniques, pp. 1050-1061, American Society of Civil Engineers, New York, 1975.

BATTJES, J.A. and J.P.F.M. JANSSEN, Energy loss and set-up due to breaking of random waves, in Proceedings 16th International Conference Coastal Engineering, pp. 569-587, American Society of Civil Engineers, New York, 1978.

DERKS, H. and M.J.F. STIVE, Field investigations in the TOW Study programme for coastal sediment transport in the Netherlands, in Proceedings of the 19th International Conference Coastal Engineering, American Society of Civil Engineers, New York, 1984.

DINGEMANS, M.W., Verification of numerical wave propagation models with field measurements; Crediz verification Haringvliet, Report W 488, Delft Hydraulics Laboratory, 1983.

STIVE, M.J.F., A scale comparison of waves breaking on a beach, Accepted for publication J. Coast. Eng., 1984.

THORNTON, E.B. and R.T. GUZA, Transformation of wave height distribution, J. Geophys. Res., 88, 5925-5938, 1983.

VAN OVEREEM, J., Morphologic behaviour of beach fill with underwater dam, Report M 1891, Delft Hydraulics Laboratory, 1983.